Immunity

Supplemental Information

The Intestinal Microbiota Contributes to the Ability of Helminths to Modulate Allergic Inflammation

Mario M. Zaiss, Alexis Rapin, Luc Lebon, Lalit Kumar Dubey, Ilaria Mosconi, Kerstin Sarter, Alessandra Piersigilli, Laure Menin, Alan W. Walker, Jacques Rougemont, Oonagh Paerewijck, Peter Geldhof, Kathleen D. McCoy, Andrew Macpherson, John Croese, Paul R. Giacomin, Alex Loukas, Tobias Junt, Benjamin J. Marsland, and Nicola L. Harris

Supplemental Data

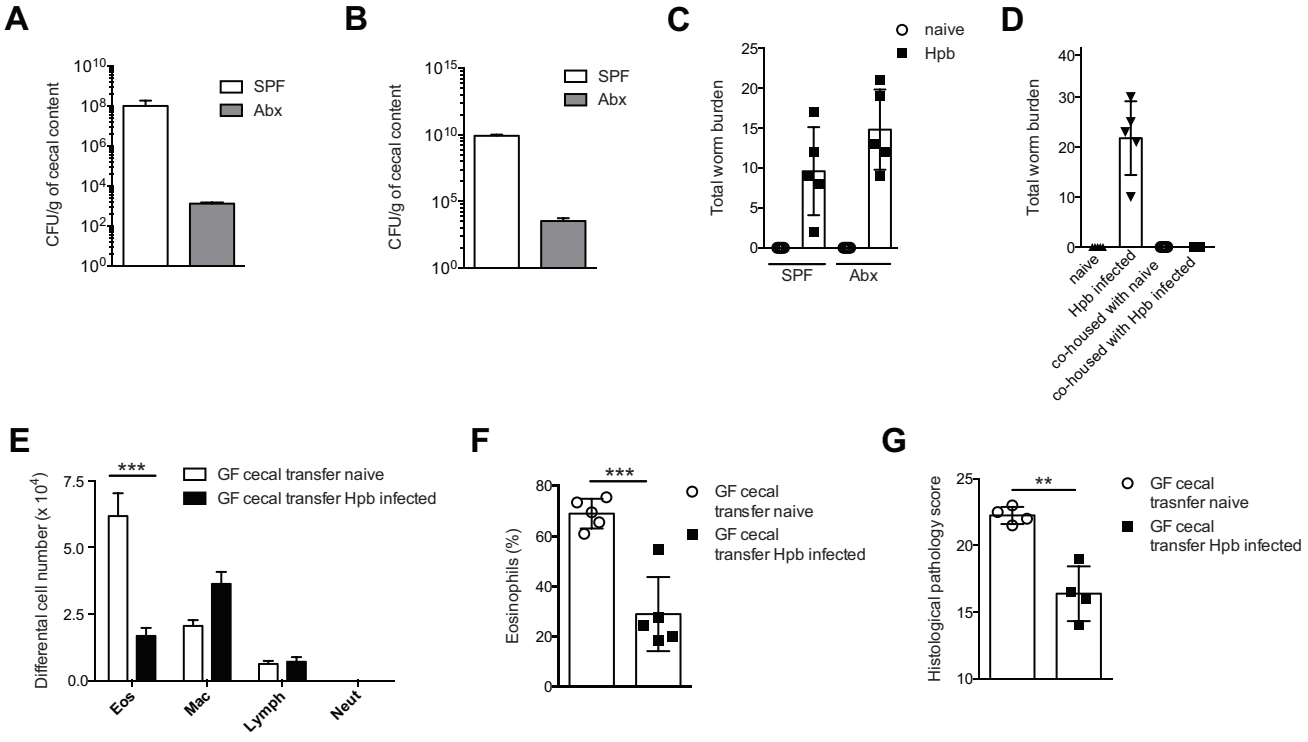

Figure S1 (related to Figure 2). Intestinal microbiota contributes to the ability of Hpb to modulate HDM-induced airway inflammation. (A-C) SPF mice were treated or not with antibiotics (Abx) and the number of (A) aerobic and (B) anaerobic colony forming units (CFUs) in cecal contents determined by bacterial plating. (C) Mice were additionally infected with Hpb and the number of adult worms in the intestine determined after 40 days. (D) Mice pretreated with antibiotics were co-housed with naive or Hpb infected SPF donors and the number of adult Hpb recovered from the intestine determined. The number of worms in both donor and recipient mice are shown. (E-G) Germ-free recipient mice were re-colonized by oral gavage with cecal contents from naive or Hpb infected donor mice. Recipients were subsequently sensitized and challenged with HDM and the ensuing allergic response determined. (E) Total differential cell counts in the BALF. (F) Percent eosinophils in BALF cells. (G) Mean gross lung histological pathology scores of H&E stained lung tissue after HDM challenges. All data are expressed as the mean +/- s.d. (n=5). Statistical significance was determined with two-way analysis of variance (ANOVA) and Student's t test. *p=0-05, **p=0-01, ***p=0.0001. Data from (A-B) are pooled from three experiments. Remaining data are from one experiment and are representative of three (C-D) or two (E-G) independent experiments.

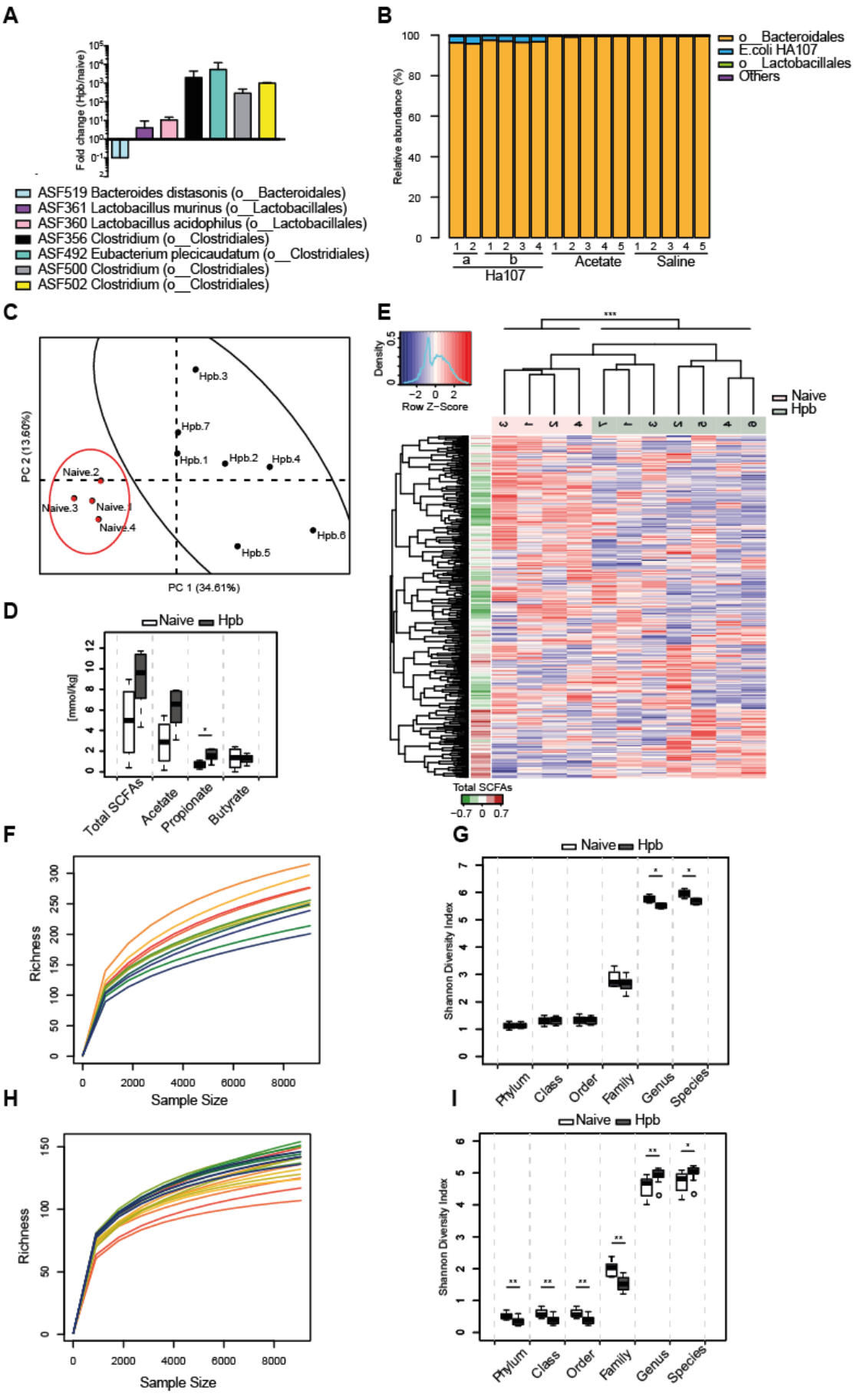
A
Fold change (Hpb/naive)
ASF519 Bacteroides distasonis (o__Bacteroidales)
ASF361 Lactobacillus murinus (o__Lactobacillales)
ASF360 Lactobacillus acidophilus (o__Lactobacillales)
ASF356 Clostridium (o__Clostridiales)
ASF492 Eubacterium plecicaudatum (o__Clostridiales)
ASF500 Clostridium (o__Clostridiales)
ASF502 Clostridium (o__Clostridiales)
B
Relative abundance (%)
o__Bacteroidales
E.coli HA107
o__Lactobacillales
Others
a
b
Ha107
Acetate
Saline
C
PC 2 (13.60%)
PC 1 (34.61%)
Hpb.3
Hpb.7
Hpb.1
Hpb.2
Hpb.4
Hpb.6
Hpb.5
Naive.2
Naive.3
Naive.1
Naive.4
D
Naive
Hpb
[mmol/kg]
Total SCFAs
Acetate
Propionate
Butyrate
E
Density
Row Z-Score
Naive
Hpb
Total SCFAs
F
Richness
Sample Size
G
Naive
Hpb
Shannon Diversity Index
Phylum
Class
Order
Family
Genus
Species
H
Richness
Sample Size
I
Naive
Hpb
Shannon Diversity Index
Phylum
Class
Order
Family
Genus
Species

Figure S2 (related to Figure 3). Hpb infection alters the cecal microbiota and increases SCFA concentrations (A) ASF mice were infected with Hpb and cecal content collected at 28 days post-infection. Data shows quantitation of ASF strains by qRT-PCR using specific primers. (B) ASF mice either received (a) $2.86x10^9$ CFU or (b) $2.15x10^3$ CFU of *E. coli* HA107 by oral gavage four weeks prior sacrifice and cecal content collection or were supplemented with 150 mM sodium acetate or 150 mM NaCl in drinking water for four weeks prior sacrifice and cecal content collection. Bacterial community composition as assessed by 16s rRNA gene sequencing is shown at the order level. (C-G) Cecal contents were collected from naive or day 40 Hpb infected SPF mice and the bacterial community was analyzed using the 16S rRNA gene sequencing method. (C) Principal coordinates analysis (PCoA) using the Bray-Curtis dissimilarity based on OTU abundances. Color clustering is based on the k-means method. Data shows individual mice. Cecal contents were collected and bacterial community was analyzed using the 16S rRNA sequencing method. (D) Cecal SCFA levels from (C). Significance determined by unpaired Student test. (E) OTU abundance heatmap from (C). The left color bar represents the Spearman correlation coefficient of each OTU with the total cecal SCFAs level. Hierarchical clustering based on the Spearman correlation coefficient was applied to order samples and OTUs. Significance determined by the Adonis method. (F) Rarefaction curves for the species richness from (C). (G) Diversity profile at multiple taxonomic levels assessed by the Shannon diversity index. (H-I) Rarefaction curves and Shannon diversity index for OTUs shown in the main Figure 3 C-E. For all data significance was determined with the Wilcoxon rank-sum test, (* $p<0.05$, ** $p<0.01$, *** $p<0.001$). Data in (A) are expressed as the mean $\pm$ s.d. (n=4-5). Data in (D, G and I) were generated using R boxplot with the middle bar representing the median and whiskers showing 1.5x Inter Quartile Range (IQR). Data are from one experiment and are representative of one (B-I) or two (A) independent experiments.

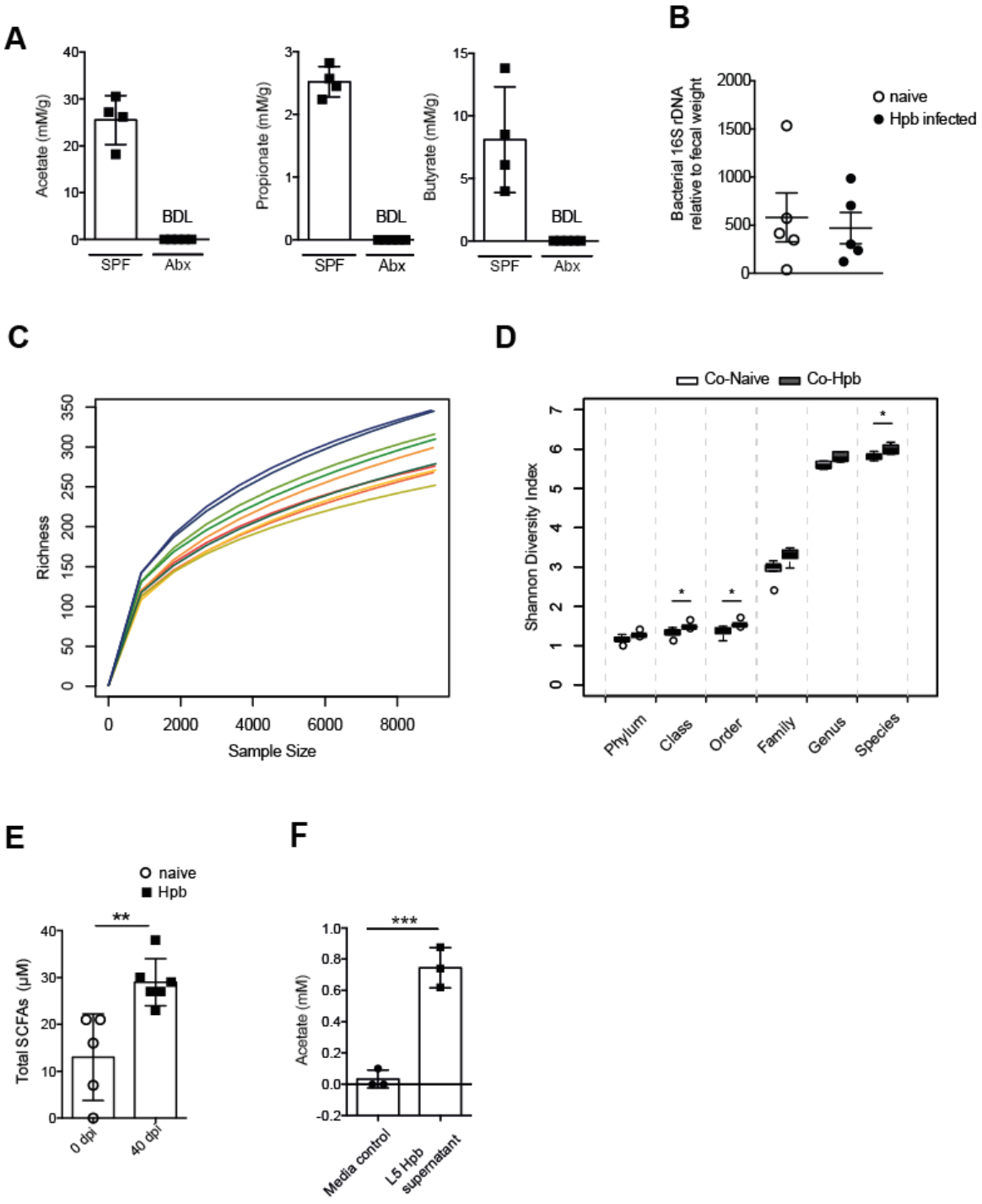
A
Acetate (mM/g)
Propionate (mM/g)
Butyrate (mM/g)
BDL
SPF
Abx
B
Bacterial 16S rDNA relative to fecal weight
naive
Hpb infected
C
Richness
Sample Size
D
Co-Naive
Co-Hpb
Shannon Diversity Index
Phylum
Class
Order
Family
Genus
Species
E
naive
Hpb
Total SCFAs (μM)
0 dpi
40 dpi
F
Acetate (mM)
Media control
L5 Hpb supernatant

Figure S3 (related to Figure 4). Hpb-induced increases in SCFA concentrations require intestinal microbial communities. (A) GC-MS quantification of SCFA acetate, propionate and butyrate levels in cecal contents of SPF and antibiotic treated (Abx) mice 40 days after infection with Hpb infective larvae. (B) RT-PCR analysis of total bacterial 16S rDNA in naive and day 40 Hpb infected mice. (C-D) Antibiotic treated recipient mice were co-housed for 3 weeks with naive SPF or Hpb infected mice and cecal contents collected and bacterial community analyzed using the 16S rRNA gene sequencing method using the same mice as depicted in Figure 4. (C) Rarefaction curves for the species richness and (D) diversity profile at multiple taxonomic levels as assessed by the Shannon diversity index. (E) GC-MS quantification of SCFA levels in the portal blood of day 40 Hpb infected and naive mice, or (F) acetate levels in in vitro cultures of adult Hpb worms. Results in (A, B, E and F) are expressed as the mean ± s.d. and statistical significance was determined with Student's t test, (* $p<0.05$, **$p<0.01$,*** $p<0.001$). For (D) data were generated using R boxplot with the middle bar representing the median and whiskers showing 1.5x Inter Quartile Range (IQR). Significance was determined with the Wilcoxon rank-sum test, (* $p<0.05$, ** $p<0.01$,*** $p<0.001$).

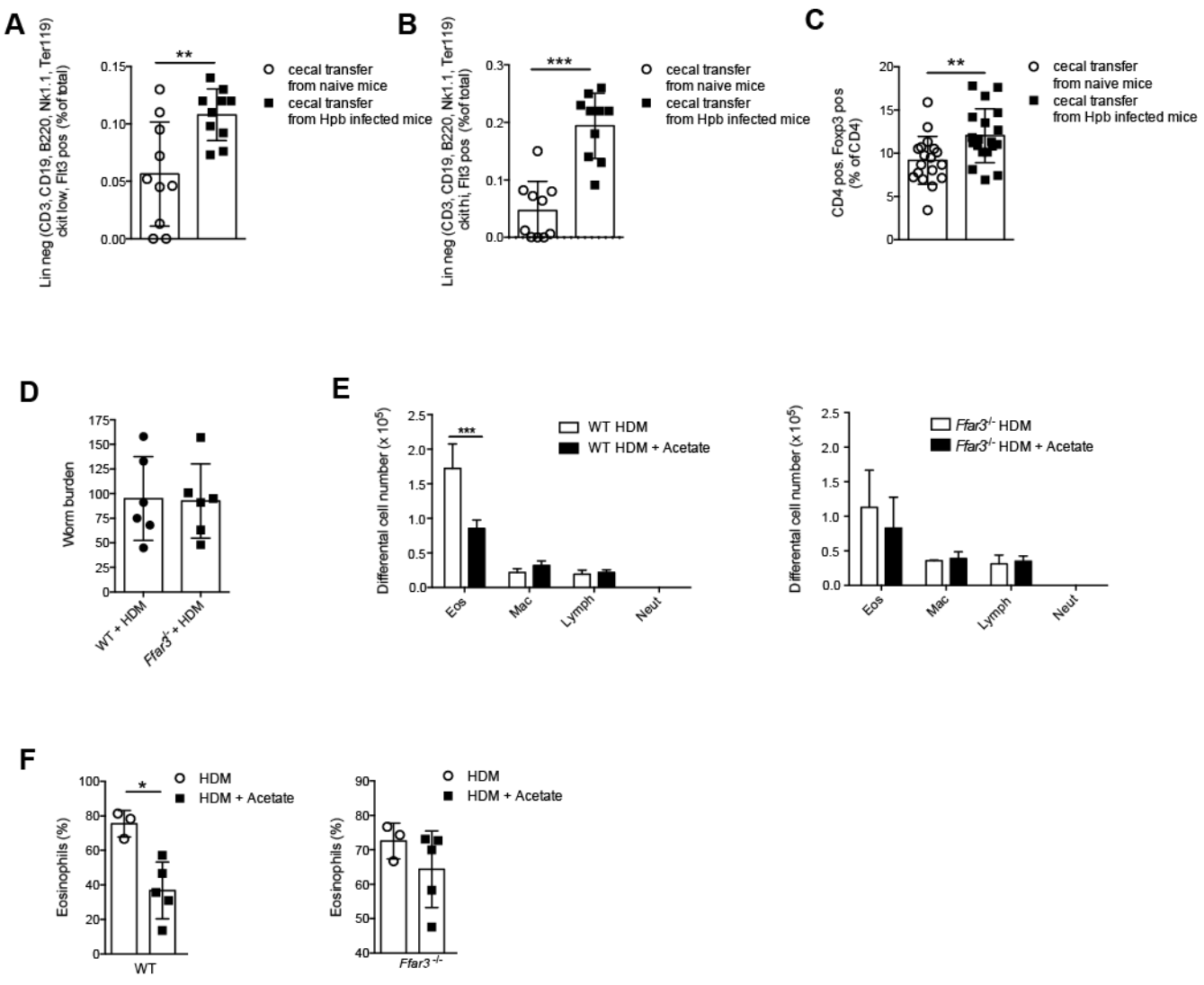

Figure S4 (related to Figure 5). SCFA-mediated attenuation of allergic airway inflammation is abrogated in *Ffar3* deficient mice. (A-C) Germ-free or antibiotic treated recipient mice were re-colonized by oral gavage of cecal contents from Hpb-infected or naive mice and 3 weeks later recipients were sensitized and challenged with HDM. Flow cytometery was used to determine the percentage of (A) common DC precursors (CDPs) and (B) macrophage and DC precursors (MDPs) in the bone marrow one day after the final HDM challenge or (C) T regs present in the lung 3 days after the final HDM challenge. (D) Wildtype or *Ffar3* deficient mice were infected with Hpb and subjected to HDM sensitization and challenge as depicted in Figure 5, and adult worms present in the intestinal lumen counted three days after the final HDM challenge. (E-F) Wildtype or *Ffar3* deficient mice were supplemented with 150 mM sodium acetate in the drinking water for four weeks then additionally subjected to HDM sensitization and challenge and BALF collected three days after the final HDM challenge. (E) Differential cell counts. Mac, macrophages; neut, neutrophils; eos, eosinophils; lymph, lymphocytes. (F) Percent eosinophils. Data in (A&B) are pooled from 2 independent experiments and data in (C) are pooled from 3 independent experiments. Data are expressed as mean ± s.d. and statistical significance determined with a Student's t test, (* $p<0.05$, ** $p<0.01$,*** $p<0.001$).

Table S1 (related to Figures 1, 2 and 5): Histological criteria for severity scoring of allergic airway inflammation.

Vasculature:

Severity	Perivascular and peribronchial/olar inflammation	Vascular hypertrophy and hyperplasia	Thickening of alveolar septa	Score (pts)
minimal	Single scattered leukocytes	Minimal thickening of the intima or media	Slightly increased cellularity	1
mild	Aggregates less than 10 cells thick	Thickening without narrowing	Alveolar wall lined by an almost continuous layer of cells	2
moderate	Aggregates about 10 cells thick	Thickening with narrowing of the lumen	Alveolar wall lined by a continuous layer of cells	3
severe	numerous coalescing aggregates more than 10 cells thick	Thickening with complete obliteration of the lumen with/without thromboemboli	Consolidation	4

Airways:

Leukocytes in alveolar spaces	Score
Absent	0
Rare cells (2-4 in 400X HPF)	1
Between 4 and 10 cells	2
More than 10 cells	3

Table S2 (related to Figures 3 and 4): Primer details used for bacterial 16S rRNA gene sequencing

	Reverse primers
	5'CAAGCAGAAGACGGCATACGAGATNNNNNNNNNNNN*AGTCAGTCAGAA***GCTGCCTCCCGTAGGAGT**3'**
	Forward primer
	5'AATGATACGGCGACCACCGAGATCTACAC*TATGGTAATTCC***AGMGTTYGATYMTGGCTCAG**3'**
	Sequencing primers
R1	5'GAGATCTACAC*TATGGTAATTCC***AGMGTTYGATYMTGGCTCAG**3'**
Index	5'**ACTCCTACGGGAGGCAGC***TTCTGACTGACT***3'
R2	5'*AGTCAGTCAGAA***GCTGCCTCCCGTAGGAGT**3'**
	Bold characters: bacteria specific 16S rRNA universal sequence F27 (forward) and R338 (reverse); Italic characters: primer pad; Italic and underlined characters: linker; Underlined characters: MID tag sequence; Thin characters: Illumina adapter.

Supplemental Experimental Procedures

Measurement of short-chain fatty acids (SCFAs)

For human SCFA analysis, frozen fecal samples were weighed into a 2 ml extraction tube. The tubes were kept in a cool rack throughout the extraction. 20 µl of internal standard (80 mM of 2-ethylbutyric acid in water, Sigma) and 200 µl of 3.2% HCl was added and samples vortexed for 1 min. 1 ml of diethyl ether was added, vortexed for 1 min and centrifuged for 3 min at 0 °C. The organic phase was transferred into a 2 ml gas chromatography (GC) vial. For the calibration curve, 100 µl of SCFA calibration standards were dissolved in water (Sigma) to concentrations of 0, 0.5, 1, 5 and 10 mM and then subjected to the same extraction procedure as the samples ($r^2 > 0.999$). All samples were run on a 7890A GC coupled to a 5975C MSD (Agilent, Palo Alto) set up with a DB-Wax, 30 m x 0.2599 x 0.2599 capillary column (Agilent). The carrier gas was helium and the column flow was 1 ml/min. The injector was set to 250 °C and the transfer line, mass spectrometry (MS) source and MS quad to 280 °C, 230 °C and 150 °C, respectively. The oven program was as follows, 50 °C initial for 1 min, then 25 °C/min to 230 °C for 10 min, with a total run time of 18 min. 1 µl of sample was injected with a split ratio of 50:1.

For mouse and pig SCFA analysis, the samples were derivatized prior to GC-MS analyses using MTBSTFA + 1 % TBDMCS as silylation reagent (Thermo Scientific). 60 µl of samples (in duplicate) were incubated with 20 µl of reagent for 1 hour at room temperature. For the calibration curve, 60 µl of the SCFA standards (acetate, propionate and butyrate) were dissolved in acetonitrile (Thermofischer) and derivatized by addition of 20 µl of reagent for 1 hour at room temperature. All samples were run on

a CP-3800 Gas Chromatograph coupled to a 1200L Quadrupole MS/MS (Varian) using a FactorFour VF-50ms, 30m x 0.25mm x 0.25mm capillary column (Varian). The carrier gas was helium and the column flow was 1 ml/min. The injector, transfer line and MS source were set to 250 °C, 250 °C and 200 °C, respectively. The oven program was as follows, 50 °C initial for 2 min, then 20 °C/min to 150 °C for 5 min, then 30 °C/min to 250 °C for 5 min. 2 µl of sample was injected and GC-MS analyses performed in duplicates. Full scan mass spectra were recorded in the 50-450 *m/z* range (1s/scan). Quantification was done by integration of the extracted ion chromatogram peaks following ion species: *m/z* 117 and 75 for acetate eluted at 5.2 min, *m/z* 131 and 75 for propionate eluted at 6.2 min, and *m/z* 145 and 75 for butyrate eluted at 6.9 min.

Bacteria quantification

Quantitative polymerase chain reaction (PCR) was performed using SYBR Green I Master Mix (Eurogentec) on a 7900HT PCR system (Applied Biosystems). Bacterial 16S rDNA and mouse 18S rDNA were amplified from total DNA using universal bacteria (Bouskra et al., 2008) and mouse-specific primers (Arizon et al., 2012). Altered Schaedler flora (ASF) species were amplified using specific primers previously described (Sarma-Rupavtarm et al., 2004).

Histology and pathology

The histopathological scoring included severity and distribution of perivascular and peribronchial/peribronchiolar inflammatory infiltrate, thickening of the alveolar septa, leukocytes in alveolar spaces as well as vascular hypertrophy and hyperplasia as detailed in Table S1. A semi-quantitative assessment of the predominant leukocyte types (eosinophils, lymphocytes, plasma cells, macrophages, etc.) in the inflammatory aggregates was also performed. The presence or absence of mucous plugs within the lumen of the bronchi and bronchiole was respectively scored with 1 and 0. The distribution of each lesion was quantified with points as follows: focal 1, multifocal 2, diffuse 3. The criteria for severity scoring of changes in the airways and vasculature are shown in Table S1. For intermediate grades of severity (such as mild to moderate, moderate to severe, etc.), 0.5 points were added to the lowest score. The total score of pulmonary damage was obtained by the sum of the single scores and is termed ‘histological pathology score’. Emphysema, atelectasis and edema were not quantified as similar changes (artifacts) were produced during the bronchoalveolar lavage. For sections stained with periodic acid-Schiff (PAS), each animal was represented by sections of the lung and five randomly selected regions from one section were evaluated (two segments of the primary conducting

airway, two segments from separate secondary conducting airways, and one segment from a tertiary conducting airway). A minimum of 100 sequential airway epithelial cells were counted from each region and the total number of PAS-positive cells per total epithelial cells was determined for each region. These regional values were then averaged to give a final PAS score per animal termed 'mean goblet cell index' (Zeki et al., 2010).

16S rRNA preparation and sequencing

DNA was first extracted from cecal content using the PowerSoil DNA isolation kit (Mo Bio Laboratories) according to manufacturer's instructions. Bacterial 16S rRNA gene V1-V2 variable regions were amplified by PCR using bar-coded primers described in Table S2 and Q5 High-fidelity PCR kit (New England Biolabs). 20 PCR cycles were performed with a template DNA input of 5 µl per 50 µl reaction mix (< 1000 ng). The temperature cycles were set as follows: 2 minutes of initial denaturing step at 98 °C, repeated steps of 30 seconds denaturing at 98 °C, 30 seconds annealing at 50 °C, 1.5 minute extension at 72 °C and a final step of 5 minutes at 72 °C. Amplicon purification was performed using the Wizard SV Gel and PCR Clean-Up System (Promega) according to manufacturer's instructions. Sequencing was performed on an Illumina MiSeq platform using MiSeq Reagent Kit v2-500 (paired-end, 2x250) with custom primers (shown in Table S2).

16S rRNA gene sequencing data analysis

Data analysis was performed using the Quantitative Insights Into Microbial Ecology (QIIME, v1.8.0) software package (Caporaso et al., 2010b) first with a closed reference OTU picking strategy, then with an open reference OTU picking strategy. Figures and statistics were generated with R (R Foundation for Statistical computing).

Low quality (< Q20) bases were truncated using Seqtk and paired end reads were merged using Fastq-join. Further quality filtering was applied and sequences were demultiplexed. Operational taxonomic units (OTUs) were picked by mapping sequences (97% similarity threshold) against a subset of the GreenGene (v13.8) sequences database filtered at 97% identity using Uclust (Haas et al., 2011). Remaining sequences were either discarded (closed reference OTU picking strategy) or clustered de-novo (open reference OTU picking strategy). Taxonomy was assigned using a pre-computed taxonomy map (closed reference OTU picking strategy) or using the Ribosomal Database Project (RDP) classifier (open reference OTU picking strategy) (Wang et al., 2007).

Starting with a closed reference OTU picking strategy, OTU tables from each experiment were

analyzed separately. OTU tables were first normalized using the rarefaction method at a depth of 9090 and calculating an average table from five random sampling repeats. OTUs representing less than 0.006% of the counts in at least one sample and present in less than 40% of the samples were discarded. Separate OTU tables were then generated for the phylum, class, order, family, genus and species (OTU) levels. Diversity was analyzed by assessing the Shannon index at multiple taxonomic levels and the richness at multiple rarefaction depths. Statistical significance was determined by Wilcoxon rank-sum test. The variance-stabilizing transformation (VST) as implemented in DESeq (Anders and Huber, 2010) was applied before comparison of experimental groups based on OTU abundances: a principal coordinates analysis (PCoA) was done using the Bray-Curtis dissimilarity based on OTU abundances and samples were clustered using the k-means method. A heat map was built based on centered and scaled OTU abundances. Samples and OTUs were ordered by hierarchical clustering using hclust based on the Spearman correlation coefficient matrix and statistical significance was determined using the permutational multivariate analysis of variance using distance matrices (Adonis method). A color bar representing the Spearman correlation coefficient of each individual OTU with SCFA levels was added.

To perform an in-depth analysis of commonalities between independent experiments, OTUs tables were generated together for all experiments using an open OTU picking strategy. To improve the taxonomic classification of OTUs assigned to poorly characterized yet relatively abundant bacterial families (Lachnospiraceae, Ruminococcaceae and S24-7), representative sequences for these families were used to build a phylogenetic tree using PyNAST (Caporaso et al., 2010a) and FastTree (Price et al., 2010) and new OTUs clusters within these families were defined based on the patristic distance and added to the original OTU taxonomy. OTU tables were then normalized using the rarefaction method at a depth of 10800 and calculating an average table from five random sampling repeats. OTUs representing less than 0.006% of the counts in at least one sample and present in less than 40% of the samples were discarded. The variance-stabilizing transformation as implemented in DESeq (Anders and Huber, 2010) was applied before comparison of experimental groups based on OTUs abundances. In each experiment, OTUs were tested for group differences by Wilcoxon rank-sum test. To highlight commonalities between experiments, OTUs showing a common fold change sign across all experiments and a significant change in at least one experiment (adjusted p-value < 0.05) were selected.

Supplemental References

Anders, S., and Huber, W. (2010). Differential expression analysis for sequence count data. Genome Biology *11*.

Arizon, M., Nudel, I., Segev, H., Mizraji, G., Elnekave, M., Furmanov, K., Eli-Berchoer, L., Clausen, B.E., Shapira, L., and Wilensky, A. (2012). Langerhans cells down-regulate inflammation-driven alveolar bone loss. Proceedings of the National Academy of Sciences *109*, 7043-7048.

Bouskra, D., Brézillon, C., Bérard, M., Werts, C., Varona, R., Boneca, I.G., and Eberl, G. (2008). Lymphoid tissue genesis induced by commensals through NOD1 regulates intestinal homeostasis. Nature *456*, 507-510.

Caporaso, J.G., Bittinger, K., and Bushman, F.D. (2010a). PyNAST: a flexible tool for aligning sequences to a template alignment. Bioinformatics *26*, 266-267.

Caporaso, J.G., Kuczynski, J., Stombaugh, J., and Bittinger, K. (2010b). QIIME allows analysis of high-throughput community sequencing data. Nature Methods *7*.

Haas, B.J., Gevers, D., Earl, A.M., and Feldgarden, M. (2011). Chimeric 16S rRNA sequence formation and detection in Sanger and 454-pyrosequenced PCR amplicons. Genome Research *21*, 494-504.

Price, M.N., Dehal, P.S., and Arkin, A.P. (2010). FastTree 2–approximately maximum-likelihood trees for large alignments. PloS One *5*.

Sarma-Rupavtarm, R.B., Ge, Z., Schauer, D.B., Fox, J.G., and Polz, M.F. (2004). Spatial distribution and stability of the eight microbial species of the altered schaedler flora in the mouse gastrointestinal tract. Applied and Environmental Microbiology *70*, 2791-2800.

Wang, Q., Garrity, G.M., and Tiedje, J.M. (2007). Naive Bayesian classifier for rapid assignment of rRNA sequences into the new bacterial taxonomy. Applied and Environmental Microbiology *73*, 5261-5267.

Zeki, A.A., Bratt, J.M., Rabowsky, M., and Last, J.A. (2010). Simvastatin inhibits goblet cell hyperplasia and lung arginase in a mouse model of allergic asthma: a novel treatment for airway remodeling? Translational Research *156*, 335-349.